



# Influence of pulverized palm kernel and egg shell additives on the hardness, coefficient of friction and microstructure of grey cast iron material for advance applications

Enesi Y. Salawu<sup>a,\*</sup>, Oluseyi O. Ajayi<sup>a</sup>, Anthony Inegbenebor<sup>a</sup>, Stephen Akinlabi<sup>b</sup>, Esther Akinlabi<sup>b</sup>

<sup>a</sup> Department of Mechanical Engineering, Covenant University, P.M.B 1023, Ota, Ogun State, Nigeria

<sup>b</sup> Department of Mechanical Engineering Science, University of Johannesburg, South Africa

## ARTICLE INFO

### Keywords:

Hardness  
Cast iron  
COF  
Microstructure

## ABSTRACT

Previous studies showed the effects of organic carbon on the mechanical properties of alloys. However, the mechanisms of graphite films formation have not been given due attention. In the present study, diffusion of carbon content via heat treatment process to produce graphite films is presented using microstructure. Consequently, the graphite films formed a protective layer on the heat treated metals which cause hardness increase and in turn improved the wear resistance of the heat treated material due to reduced coefficient of friction. The excellent tribological properties of carburized grey cast iron showed the potentials of palm kernel and egg shell for advance material modifications.

## Introduction

The increasing demand for super hard alloys or materials for advanced engineering applications necessitates the need for development of materials of superior mechanical properties [1]. Application of nanoparticles to cast iron modification has increased its applications in gear, bearings, sprockets and housings. Recently, studies have revealed that it is possible to simulate the behaviour of these nanoparticles using Buongiorno's model as they interact with the substrate [2–4]. Thus, the volumetric fractions as well as the heat transfer rate of the nanoparticles which have great effects on the mechanical properties can be determined [5–7]. Despite significance of cast iron, it is limited in areas involving chemical applications due to the corrosive nature of such environment [8]. Thus, this study investigates the influence of pulverized organic carbon (Palm kernel shell and egg shell) on the mechanical properties of grey cast iron material for advance applications.

## Materials and method

Pulverized palm kernel shell and egg shell were obtained for this study. Grey cast iron materials of dimensions (20 mm × 20 mm × 10 mm) and chemical composition (wt.%) of 2.68C, 1.42 Si, 0.63 Mn, 0.13 S,

0.28 P were equally prepared using different grades of silicon carbide abrasives to obtain a polished and smooth surface for easy carbon penetration. Carburization process was employed for the heat treatment. A mixing ratio of 70 (wt.%) of pulverized palm kernel shell and 30 (wt.%) of pulverized egg shell based on Voige law of mixture was used for the experiment while each sample was embedded into a stainless container and loaded into a muffle furnace of 1200 °C capacity. The carburization was carried at 900 °C for 60 minutes respectively. Scanning electron microscope with Energy Dispersive Spectroscopy was used to characterize the microstructure, while Vickers' hardness tester and sliding wear tester were used to determine the hardness and coefficient of friction of the heat treated grey cast iron material.

## Results and conclusion

Figs. 1 and 2 SEM/EDS morphology of the carburized sample and variation in coefficient of friction and force with time respectively, while Tables 1–3 presents the chemical composition of as-received and carburized cast iron as well as their micro-hardness properties.

From Fig. 1, it could be observed from the SEM image that graphite films were deposited at the metal interface due to the diffused carbon content at 900 °C for 60 minutes. The graphite deposits formed a

\* Corresponding author.

E-mail address: [enesi.salawu@covenantuniversity.edu.ng](mailto:enesi.salawu@covenantuniversity.edu.ng) (E.Y. Salawu).

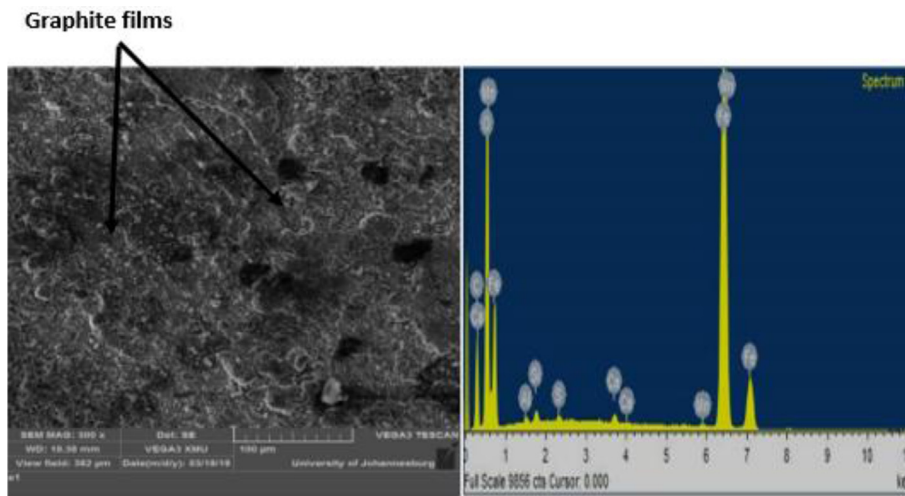


Fig. 1. SEM/EDS Morphology of Carburized sample at 900 °C for 60 minutes.

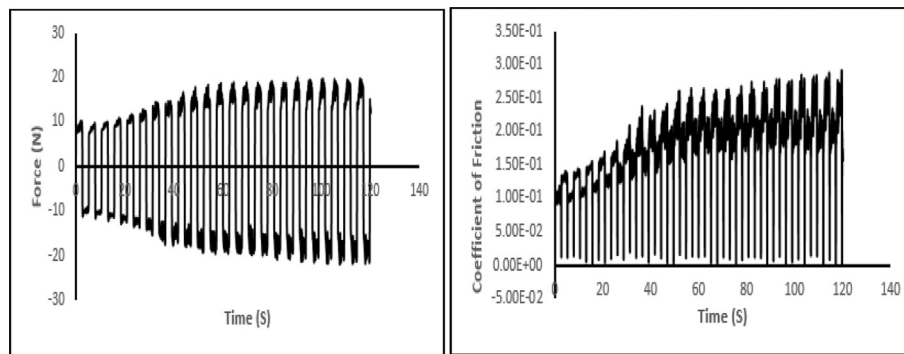


Fig. 2. Variation of Force and Coefficient of Friction with time for Carburized sample at 900 °C for 60 minutes.

Table 1

Composition of as-received grey cast iron material.

Elements	Carbon	Iron	Silicon	Manganese	Sulphur	Phosphorus
Composition (%)	2.68	84.3	1.42	0.63	0.13	0.28

Table 2

Composition of carburized grey cast iron material.

Elements	Carbon	Iron	Silicon	Manganese	Sulphur	Phosphorus
Composition (%)	5.40	86.81	1.87	0.3715	0.499	0.382

protective layer at the metallic surface. Consequently, the percentage of manganese present in the structure depicts that there was pearlite formation due to austenitic transformation, thus resulting to excellent hardness increase and strength. Further to this, silicon presence in the microstructure would improve the wear properties of the heat treated grey cast iron. Additionally, Fig. 2 showed the variation of force with time during sliding wear test. The peak variation indicates the dynamic response of the heat treated sample which is traceable to improved hardness. More so, the frictional force was observed to have values of 0.0000796, 0.0000438 and later increased to a 0.086 and 0.10. The low

friction observed at the initial stage of sliding was due to presence of oxide films and moisture at the interface of the test material [9]. Thus, the low friction was traceable to the high hardness value obtained from palm kernel shell powder.

**Conflict of interest**

None.

**Acknowledgement**

The authors appreciate the management of Covenant University, Nigeria for the part sponsorship of this research work.

Table 3

Micro-hardness properties.

As-received Grey Cast Iron Material	116.9 Hv
Carburized Grey Cast Iron Material	355.8 Hv

## References

- [1] E.Y. Salawu, O.O. Ajayi, A.O. Inegbenebor, Turbulence flow simulation of Molten metals in runners for defect control in casting of a spur gear blank, *Int. J. Mech. Eng. Technol.* (2019) 1921–1933.
- [2] A. Wakif, Z. Boualahia, R. Sehaqui, A semi-analytical analysis of electro-thermo-hydrodynamic stability in dielectric nanofluids using Buongiorno's mathematical model together with more realistic boundary conditions, *Res. Phys.* 9 (2018) 1438–1454.
- [3] A. Wakif, Z. Boualahia, S.R. Mishra, M.M. Rashidi, R. Sehaqui, Influence of a uniform transverse magnetic field on the thermo-hydrodynamic stability in water-based nanofluids with metallic nanoparticles using the generalized Buongiorno's mathematical model, *Euro. Phys. J. Plus* 133 (5) (2018) 181.
- [4] A. Wakif, Z. Boualahia, A. Amine, I.L. Animasaun, M.I. Afridi, M. Qasim, R. Sehaqui, Magneto-convection of alumina-water nanofluid within thin horizontal layers using the revised generalized Buongiorno's model, *Front. Heat Mass Trans. (FHMT)* 12 (2018).
- [5] A. Wakif, Z. Boualahia, R. Sehaqui, Numerical study of the onset of convection in a Newtonian nanofluid layer with spatially uniform and non-uniform internal heating, *J. Nanofluids* 6 (1) (2017) 136–148.
- [6] A. Wakif, Z. Boualahia, R. Sehaqui, Numerical analysis of the onset of longitudinal convective rolls in a porous medium saturated by an electrically conducting nanofluid in the presence of an external magnetic field, *Res. Phys.* 7 (2017) 2134–2152.
- [7] A. Wakif, Z. Boualahia, F. Ali, M.R. Eid, R. Sehaqui, Numerical analysis of the unsteady natural convection MHD Couette nanofluid flow in the presence of thermal radiation using single and two-phase nanofluid models for Cu–Water nanofluids, *Int. J. Algorithms Comput. Math.* 4 (3) (2018) 81.
- [8] S.A. Afolalu, O.P. Abioye, E.Y. Salawu, I.P. Okokpujie, A.A. Abioye, O.A. Omotosho, O.O. Ajayi, Impact of heat treatment on HSS cutting tool (ASTM A600) and its behaviour during machining of mild steel (ASTM A36), in: *AIP Conference Proceedings*, vol. 1957, AIP Publishing, 2018, April, p. 050003.
- [9] E.E.T. ELSawy, M.R. EL-Hebeary, I.S.E. El Mahallawi, Effect of manganese, silicon and chromium additions on microstructure and wear characteristics of grey cast iron for sugar industries applications, *Wear* 390 (2017) 113–124.